

An exponential approximation for continuum percolation in dipolar hard-sphere fluids

This article has been downloaded from IOPscience. Please scroll down to see the full text article.

1996 J. Phys.: Condens. Matter 8 1857

(<http://iopscience.iop.org/0953-8984/8/12/002>)

View [the table of contents for this issue](#), or go to the [journal homepage](#) for more

Download details:

IP Address: 171.66.16.208

The article was downloaded on 13/05/2010 at 16:25

Please note that [terms and conditions apply](#).

An exponential approximation for continuum percolation in dipolar hard-sphere fluids

C Manuel Carlevaro[†], César Stoico[†] and Fernando Vericat^{‡§}

[†] Facultad de Ciencias Bioquímicas y Farmacéuticas, Universidad Nacional de Rosario, Rosario, Argentina

[‡] Instituto de Física de Líquidos y Sistemas Biológicos (IFLYSIB)-UNLP-CONICET, cc 565 - (1900) La Plata, Argentina

[§] Grupo de Aplicaciones Matemáticas y Estadísticas de la Facultad de Ingeniería, (GAMEFI), Departamento de Fisicomatemática, Facultad de Ingeniería, Universidad Nacional de La Plata, La Plata, Argentina

Received 6 November 1995

Abstract. We consider a generalized mean spherical approximation for the pair-connectedness function of a dipolar hard-sphere fluid. Based on its analytical solution, we propose an exponential approach to the continuum percolation of dipolar fluids. The mean cluster size and the critical percolation density so obtained agree well with previously reported Monte Carlo simulations. The Kirkwood g_K factor calculated among connected dipoles, a magnitude that can be taken as a measure of the dipolar ordering inside the cluster, also compares well with the simulation results.

1. Introduction

The notion of percolation has been widely used to study a variety of phenomena which are characterized by qualitative changes in the macroscopic behaviour of the systems involved. These changes can be associated with a remarkable increase in the size of the clusters formed by the atoms or molecules of the systems. Thus, application of percolation concepts to the understanding of phenomena such as nucleation [1], gelation [2], spinodal decomposition [3], water structure [4], the conductor–insulator transition in liquid metals [5] and conduction in disordered materials [6] have been very common in the last few years. Recently, and more directly related to our own interests here, Feldman *et al* [7] have used percolation arguments to explain the dielectric behaviour of microemulsions.

Theoretical percolation studies have been basically oriented in two directions: percolation in lattice systems (see e.g. [8]) and percolation in continuum systems. The latter approach has a wide field of applications in fluids and disordered systems and is that which will be followed in this work.

Percolation is closely related to clustering and, within the framework of Hill's theory [9], physical clusters are defined by some connectivity criterion. A central role is played by the pair-connectedness function $\rho^{\dagger}(\mathbf{1}, \mathbf{2})$ that very properly describes the particle distribution inside the clusters. This function, introduced some time ago by Coniglio and collaborators [10, 11], represents the probability density of having two molecules in differential elements $d\mathbf{1}$ and $d\mathbf{2}$ around their coordinates specified by $\mathbf{1}$ and $\mathbf{2}$, respectively, with the condition that both molecules belong to the same cluster. Unfortunately, the pair-connectedness

function is not directly measurable. However it is a very useful tool in understanding the clustering properties of several systems. In order to obtain it computer simulations or some theoretical treatment become indispensable. Both theoretical and simulation approaches have been intensively used in recent years to study clustering and continuum percolation of model fluids. Among the theoretical methods we mention the connectedness version of integral equations [12] such as the Percus–Yevick [13]–[16] and the mean spherical approximation (MSA) [17] and also series expansions [11], [18], [19]. Simulation methods include molecular dynamics [20] and Monte Carlo runs [21]–[26].

Integration of the pair-connectedness function over the whole available space yields the mean cluster size, the divergence of which guarantees the existence of a percolation transition [10]. The system density at which the percolation occurs is called the critical or threshold density and will be denoted ρ_c . Unlike the pair-connectedness function ρ_c can be determined from experiment by establishing the density at which the value of a certain physical quantity experiences a drastic change [27].

Pair-connectedness functions, mean cluster sizes, critical percolation densities and several other related properties, have been calculated using the above theories for a variety of systems: randomly centred spheres [13], [14], [21], [22]; adhesive spheres [13], [23], extended neutral hard spheres [15], [25], [25] and hard spheres with square-wells [16], [26] and Yukawa tails [17]. In all these systems, the particles interact among themselves via spherically symmetric pair potentials (i.e. atomic fluids). However, many interesting features of clustering and percolation in molecular liquids are due to the anisotropy in the intermolecular forces.

In previous work, the percolation problem for a system with orientation-dependent interactions, namely a dipolar-hard-sphere fluid, has been addressed through Monte Carlo simulation and connectedness theory [28], [29].

In particular [28] pointed out that linear theories, such the mean spherical approximation, are not suitable for studying clustering and percolation of dipolar hard spheres since the orientation-averaged pair-connectedness functions do not depend on the dipole moment and hence the mean cluster size these theories give are the same as for simple hard spheres (without dipoles embedded), as is seen in figure 1 below. In order to obtain mean cluster sizes which do depend on the dipolar moment, we propose two exponential approaches in that work. One of them is the connectedness version of the perturbation theory of Andersen and Chandler [30], which is based in the MSA connectedness pair correlation function. The second exponential approach was obtained by retaining just the connectedness part of the total pair correlation function in the perturbation theory, developed by Gubbins and Gray [31], known as the first-order y -expansion.

In [29], we performed Monte Carlo simulations for two models of dipolar fluids: (i) a system of hard spheres with an embedded point dipole, say the same model we are interested in here; (ii) a related system of hard spheres in which the dipole–dipole forces are replaced by an angular-averaged dipolar potential. The simulation results show that clusters become larger in size and acquire a stronger mean dipolar moment when the particles' dipolar moments are increased. Far from the percolation transition, the clusters are non spherical, the eccentricity being favoured by the energetic of dipolar orientation. Furthermore, they reveal that larger dipolar strengths imply smaller percolation densities.

In the same work the simulation data were compared with theoretical results obtained from two different theories. The connectedness first-order y -expansion of Gubbins and Gray was applied to model (i), whereas the connectedness version of the Percus–Yevick integral equation was used for model (ii). This last theory reproduces the corresponding Monte Carlo results rather well. However it is unable to describe some interesting features

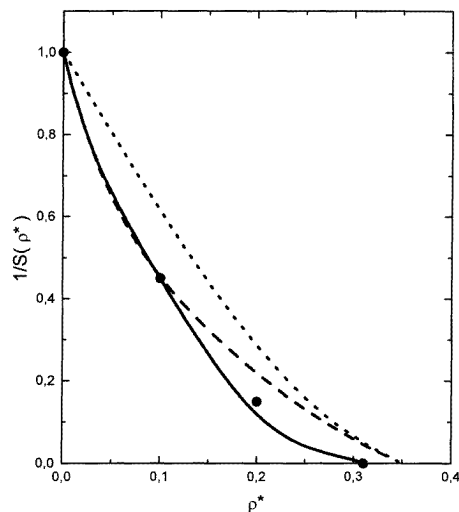


Figure 1. Inverse mean cluster size versus reduced density from the connectedness MSA (dotted line), the MSA-based EXP approximation (dashed line) and the GMSA-based EXP approximation (full line) for a dipolar hard spheres system with $\mu^{*2} = 2.0$ and connectivity distance $d = 1.25\sigma$. Monte Carlo data (full circles) are from [29].

that have directly to do with the dipoles relaxation. Instead the y -expansion was applied to a model where the dipole fluctuations in orientation are explicitly taken into account, but the comparison with simulation data gives poorer results. Thus, for example, although the mean cluster size it gives is dipole dependent, the critical percolation density is not, giving the same ρ_c whatever the dipolar moment is.

Here we consider, for the dipolar hard-sphere model, the first one of the exponential approaches introduced in [28], namely the connectedness form of the Andersen and Chandler perturbation theory. Yet this approach has the same deficiency as the y -expansion i.e. the ρ_c is not affected by the dipolar perturbation. In order to overcome this undesirable feature, we improve the theory by considering a generalized mean spherical approximation (GMSA) [32] for the spherical part of the pair correlation function, where the parameters are adjusted in such a way that at contact the pair correlation functions and their first derivative verify the quadratic hypernetted chain (QHNC) closure for dipolar hard spheres [33].

2. Theory

2.1. The model

We consider the standard model of a dipolar hard-sphere (DHS) fluid, namely an assembly of hard spheres of diameter σ with a point dipole of dipolar moment μ at their centres. We assume that there are N such molecules in volume V , so that the number density is $\rho = N/V$.

We denote the coordinates of a given molecule labelled i by $i \equiv (\mathbf{r}_i, \hat{\Omega}_i)$, where \mathbf{r}_i is the position of the sphere centre and $\hat{\Omega}_i$ gives the orientation of the point dipole. Two dimensionless parameters characterize the system: the reduced density $\rho^* = \rho\sigma^3$ and the reduced dipolar moment $\mu^{*2} = \beta\mu^2/\sigma^3$ where, as usual, β denotes the Boltzmann thermal factor.

The pair potential between any two particles **1** and **2** is

$$V(\mathbf{1}, \mathbf{2}) = \begin{cases} \infty & r_{12} < \sigma \\ -(\mu^2/r_{12}^3)[3(\hat{\Omega}_1 \cdot \hat{\mathbf{r}}_{12})(\hat{\Omega}_2 \cdot \hat{\mathbf{r}}_{12}) - (\hat{\Omega}_1 \cdot \hat{\Omega}_2)] & r_{12} > \sigma \end{cases} \quad (1)$$

Here r_{12} is the magnitude and \hat{r}_{12} is the direction of the vector difference $\mathbf{r}_{12} = \mathbf{r}_1 - \mathbf{r}_2$.

The model description is completed by giving a cluster definition. As pointed out by Hill [9], the particular cluster definition is arbitrary for thermodynamic purposes, provided it only specifies the way in which the molecular phase space gets partitioned into regions that determine, without ambiguity, the participation of molecules in clusters.

Here we consider that two molecules belong to the same cluster if they are connected. In order to define our connectedness criterion, we consider a ‘connectivity distance’ d , so that two spheres are directly connected if they are separated by a distance smaller than d . Moreover, two spheres are taken as indirectly connected if they are linked by a path of directly connected spheres, and as connected in general if they are either directly or indirectly connected. Thus our cluster definition is equivalent to requiring connectivity between each pair of molecules belonging to the cluster.

2.2. Pair-connectedness functions and mean cluster size

According to the previous cluster definition, the appropriate effective pair potentials between connected and disconnected molecules are [9]

$$V^\dagger(\mathbf{1}, \mathbf{2}) = \begin{cases} V(\mathbf{1}, \mathbf{2}) & r_{12} < d \\ \infty & r_{12} > d \end{cases} \quad (2)$$

and

$$V^*(\mathbf{1}, \mathbf{2}) = \begin{cases} \infty & r_{12} < d \\ V(\mathbf{1}, \mathbf{2}) & r_{12} > d \end{cases} \quad (3)$$

respectively, where d is the characteristic connectivity distance.

Following Hill [9], the Boltzmann factor $e(\mathbf{1}, \mathbf{2}) \equiv \exp[-\beta V(\mathbf{1}, \mathbf{2})]$ can be split into ‘connectedness’ and ‘blocking’ terms

$$e(\mathbf{1}, \mathbf{2}) = e^\dagger(\mathbf{1}, \mathbf{2}) + e^*(\mathbf{1}, \mathbf{2}) \quad (4)$$

where

$$e^\dagger(\mathbf{1}, \mathbf{2}) = \exp[-\beta V^\dagger(\mathbf{1}, \mathbf{2})] \quad (5)$$

and

$$e^*(\mathbf{1}, \mathbf{2}) = \exp[-\beta V^*(\mathbf{1}, \mathbf{2})]. \quad (6)$$

Since $e(\mathbf{1}, \mathbf{2})$ is the statistical weight in the configurational integrals, the pair functions can be separated in a way similar to that given by equation (4). In particular, the total and the direct correlation functions are written

$$h(\mathbf{1}, \mathbf{2}) = h^\dagger(\mathbf{1}, \mathbf{2}) + h^*(\mathbf{1}, \mathbf{2}) \quad (7)$$

$$c(\mathbf{1}, \mathbf{2}) = c^\dagger(\mathbf{1}, \mathbf{2}) + c^*(\mathbf{1}, \mathbf{2}) \quad (8)$$

The connectedness total-correlation function $h^\dagger(\mathbf{1}, \mathbf{2})$ is related to the connectedness correlation function $\rho^\dagger(\mathbf{1}, \mathbf{2})$ according to $\rho^\dagger(\mathbf{1}, \mathbf{2}) = (\rho/4\pi)[h^\dagger(\mathbf{1}, \mathbf{2}) + 1]$.

In terms of $h^\dagger(\mathbf{1}, \mathbf{2})$, the mean cluster size is defined as

$$\begin{aligned} S(\rho) &= 1 + \frac{\rho}{V} \int d\mathbf{1} d\mathbf{2} h^\dagger(\mathbf{1}, \mathbf{2}) \\ &= 1 + 4\pi\rho \int_0^\infty dr_{12} r_{12}^2 \langle h^\dagger(\mathbf{1}, \mathbf{2}) \rangle_{\hat{\Omega}_1, \hat{\Omega}_2}. \end{aligned} \quad (9)$$

where $\langle h^\dagger(\mathbf{1}, \mathbf{2}) \rangle_{\hat{\Omega}_1, \hat{\Omega}_2}$ denotes the unweighted angular average of $h^\dagger(\mathbf{1}, \mathbf{2})$.

The critical density ρ_c verifies

$$\lim_{\rho \rightarrow \rho_c} S(\rho) = \infty. \quad (10)$$

This equation expresses, in mathematical language, the meaning of ρ_c ; the density at which a macroscopic fraction of molecules first become connected.

2.3. Connectedness MSA

The connectedness mean spherical approximation is defined by the connectedness Ornstein–Zernike relation

$$h^\dagger(\mathbf{1}, \mathbf{2}) = c^\dagger(\mathbf{1}, \mathbf{2}) + \frac{\rho}{4\pi} \int d\mathbf{3} h^\dagger(\mathbf{1}, \mathbf{3}) c^\dagger(\mathbf{3}, \mathbf{2}) \quad (11)$$

with the closures

$$h^\dagger(\mathbf{1}, \mathbf{2}) = h(\mathbf{1}, \mathbf{2}) + 1 \quad r_{12} < d \quad (12)$$

and

$$c^\dagger(\mathbf{1}, \mathbf{2}) = 0 \quad r_{12} > d. \quad (13)$$

In these equations $h^\dagger(\mathbf{1}, \mathbf{2})$ and $c^\dagger(\mathbf{1}, \mathbf{2})$ are, the total and direct connectedness pair correlation functions respectively. We use Wertheim's MSA solution [34] for $h(\mathbf{1}, \mathbf{2})$ in equation (12). The solution is expanded in terms of the following three rotational invariants

$$\begin{aligned} \Phi^{000}(\mathbf{1}, \mathbf{2}) &= 1 \\ \Phi^{110}(\mathbf{1}, \mathbf{2}) &= -3^{1/2}(\hat{\Omega}_1 \cdot \hat{\Omega}_2) \\ \Phi^{112}(\mathbf{1}, \mathbf{2}) &= (3/10)^{1/2}[3(\hat{\Omega}_1 \cdot \hat{r}_{12})(\hat{\Omega}_2 \cdot \hat{r}_{12}) - (\hat{\Omega}_1 \cdot \hat{\Omega}_2)] \end{aligned} \quad (14)$$

where the notation of Blum [35] has been used. Therefore, the connectedness functions $h^\dagger(\mathbf{1}, \mathbf{2})$ and $c^\dagger(\mathbf{1}, \mathbf{2})$ also have a similar invariant expansion

$$f^\dagger(\mathbf{1}, \mathbf{2}) = f^{\dagger 000}(r_{12})\Phi^{000}(\mathbf{1}, \mathbf{2}) + f^{\dagger 110}(r_{12})\Phi^{110}(\mathbf{1}, \mathbf{2}) + f^{\dagger 112}(r_{12})\Phi^{112}(\mathbf{1}, \mathbf{2}) \quad (15)$$

with $f^\dagger \equiv h^\dagger$ or c^\dagger .

With this expression for $h^\dagger(\mathbf{1}, \mathbf{2})$ and $c^\dagger(\mathbf{1}, \mathbf{2})$, the integral equation given by equations (11)–(13) decouples into three independent integral equations. One of them is for the radial functions $f^{\dagger 000}(r_{12})$ and the other two are for two auxiliary radial functions which are functionals of $f^{\dagger 110}(r_{12})$ and $f^{\dagger 112}(r_{12})$. Each one of these three integral equations can be analytically solved using Baxter's factorization technique. For details the reader is referred to [28]. In particular, there it is shown that the first of these integral equations corresponds to the connectedness MSA for just hard spheres (without dipoles) [15]. Therefore, the mean cluster size as given by equation (9) does not depend on the dipole strength. Moreover, it is the same as that for simple extended hard spheres:

$$S^{MSA}(\rho) = 1 + 4\pi\rho \int_0^\infty dr_{12} r_{12}^2 \cdot h^{\dagger 000}(r_{12}) \quad (16)$$

since $h^{\dagger 000}(r_{12})$ is the pair-connectedness function for extended hard spheres of diameter σ and a connectivity distance d .

The dotted curve in figure 1 gives the inverse of the mean cluster size for the dipolar hard sphere model $1/S^{MSA}(\rho)$, calculated in the MSA, as a function of the system density ρ and should be compared against the 'exact result' given by the Monte Carlo simulation points reported in [29]. The reduced dipolar moment is $\mu^{*2} = 2.0$ and the connectivity distance is $d = 1.25\sigma$. As already mentioned, this curve is the same as that calculated by DeSimone *et al* [15] for extended hard spheres.

3. Exponential approaches

3.1. MSA-based EXP approximation

In order to overcome the undesirable fact of having a dipolar-independent mean cluster size, in [28] we have considered a connectedness exponential approximation (EXP) that is based on the perturbation theory of Andersen and Chandler [30], [36]. In the theory, the complete pair potential (equation (1)) is separated:

$$V(\mathbf{1}, \mathbf{2}) = V_0(\mathbf{1}, \mathbf{2}) + V_1(\mathbf{1}, \mathbf{2}) \quad (17)$$

with

$$V_0(\mathbf{1}, \mathbf{2}) = V^{000}(r_{12}) = \begin{cases} \infty & r_{12} < \sigma \\ 0 & r_{12} > \sigma \end{cases} \quad (18)$$

(the reference potential) and

$$V_1(\mathbf{1}, \mathbf{2}) = -(10/3)^{1/2}(\mu^2/r_{12}^3)\Phi^{112}(\mathbf{1}, \mathbf{2}) \quad (19)$$

the dipolar interaction. Thus, the total pair correlation functions are written

$$h(\mathbf{1}, \mathbf{2}) = h_0(r_{12}) + h_1(\mathbf{1}, \mathbf{2}) \quad (20)$$

The functions $h_0(r_{12})$ and $h_1(\mathbf{1}, \mathbf{2})$ verify $\langle h(\mathbf{1}, \mathbf{2}) \rangle_{\hat{\Omega}_1, \hat{\Omega}_2} = h_0(r_{12})$ and $\langle h_1(\mathbf{1}, \mathbf{2}) \rangle_{\hat{\Omega}_1, \hat{\Omega}_2} = 0$.

The exponential approximations we consider can formally be derived from the exact relationship [36], [37]

$$g(\mathbf{1}, \mathbf{2}) = g_0(r_{12}) \exp[-\beta V_1(\mathbf{1}, \mathbf{2})] \exp[h_1(\mathbf{1}, \mathbf{2}) - c_1(\mathbf{1}, \mathbf{2}) + d(\mathbf{1}, \mathbf{2})] \quad (21)$$

Here, $c_1(\mathbf{1}, \mathbf{2})$ is the angle-dependent part of the direct correlation function and $d(\mathbf{1}, \mathbf{2})$ denotes elementary diagrams.

Taking $d(\mathbf{1}, \mathbf{2}) = 0$ and using the MSA expressions for $h_1(\mathbf{1}, \mathbf{2})$ and $c_1(\mathbf{1}, \mathbf{2})$, we obtain the EXP approximation of Andersen and Chandler [30]

$$g(\mathbf{1}, \mathbf{2}) = g_{0MSA}(r_{12}) \exp[h_{1MSA}(\mathbf{1}, \mathbf{2})] \quad (22)$$

where $g_{0MSA}(r_{12}) = g_{MSA}^{000}(r_{12})$ and

$$h_{1MSA}(\mathbf{1}, \mathbf{2}) = h_{MSA}^{110}(r_{12})\Phi^{110}(\mathbf{1}, \mathbf{2}) + h_{MSA}^{112}(r_{12})\Phi^{112}(\mathbf{1}, \mathbf{2}). \quad (23)$$

In order to obtain equation (22) we have taken into account that, in the MSA, $c_0(r_{12}) = 0$ and $c_1(\mathbf{1}, \mathbf{2}) = -\beta V_1(\mathbf{1}, \mathbf{2})$ for $r_{12} > \sigma$.

The connectedness version of the approximation in equation (22) we have proposed in [28] is

$$\begin{aligned} [h_{EXP}^\dagger(\mathbf{1}, \mathbf{2})]_{MSA} &= g_{MSA}^{\dagger 000}(r_{12}) \exp[h_{1MSA}(\mathbf{1}, \mathbf{2})] + \left[g_{MSA}^{000}(r_{12}) \right. \\ &\quad \left. - g_{MSA}^{\dagger 000}(r_{12}) \right] \left\{ \exp[h_{1MSA}^\dagger(\mathbf{1}, \mathbf{2})] - 1 \right\} \end{aligned} \quad (24)$$

with $h_{1MSA}(\mathbf{1}, \mathbf{2})$ giving by equation (23) and $h_{1MSA}^\dagger(\mathbf{1}, \mathbf{2})$ the connectedness part of $h_{1MSA}(\mathbf{1}, \mathbf{2})$

$$h_{1MSA}^\dagger(\mathbf{1}, \mathbf{2}) = h_{MSA}^{\dagger 110}(r_{12})\Phi^{110}(\mathbf{1}, \mathbf{2}) + h_{MSA}^{\dagger 112}(r_{12})\Phi^{112}(\mathbf{1}, \mathbf{2}). \quad (25)$$

In going from equation (22) to equation (24), the further approximation $\{\exp[h_{1MSA}(\mathbf{1}, \mathbf{2})]\}^\dagger \simeq \exp[h_{1MSA}^\dagger(\mathbf{1}, \mathbf{2}) - 1]$ was made. This approximation implies discarding all the diagrams in $\{\exp[h_{1MSA}(\mathbf{1}, \mathbf{2})]\}^\dagger$ which are not products of diagrams in $h_{1MSA}^\dagger(\mathbf{1}, \mathbf{2})$ [28].

The replacement of $h^\dagger(\mathbf{1}, \mathbf{2})$ in equation (9) by equation (24) gives the mean cluster size. The involved integrations are greatly simplified if use is made of the invariant expansion for the exponentials of tensorial expressions reported by Blum and Torruella [38]. We obtain

$$(S^{EXP})_{MSA}(\rho) = 1 + 4\pi\rho \int_0^\infty dr_{12} r_{12}^2 \langle [h_{EXP}^\dagger(\mathbf{1}, \mathbf{2})]_{MSA} \rangle_{\hat{\Omega}_1, \hat{\Omega}_2} \quad (26)$$

where

$$\begin{aligned} \langle [h_{EXP}^\dagger(\mathbf{1}, \mathbf{2})]_{MSA} \rangle_{\hat{\Omega}_1, \hat{\Omega}_2} &= g_{MSA}^{\dagger 000}(r_{12}) i_0^{00} \{h_{MSA}^0(r_{12}); h_{MSA}^1(r_{12})\} \\ &+ [g_{MSA}^{000}(r_{12}) - g_{MSA}^{\dagger 000}(r_{12})] i_0^{00} \{h_{MSA}^{\dagger 0}(r_{12}); h_{MSA}^{\dagger 1}(r_{12})\}. \end{aligned} \quad (27)$$

Here

$$\begin{aligned} h_{MSA}^{\dagger 0}(r_{12}) &= (1/3)^{1/2} h_{MSA}^{\dagger 110}(r_{12}) - (2/15)^{1/2} h_{MSA}^{\dagger 112}(r_{12}) \\ h_{MSA}^{\dagger 1}(r_{12}) &= -(1/3)^{1/2} h_{MSA}^{\dagger 110}(r_{12}) - (1/30)^{1/2} h_{MSA}^{\dagger 112}(r_{12}) \end{aligned} \quad (28)$$

and the corresponding expressions for $h_{MSA}^0(r_{12})$ and $h_{MSA}^1(r_{12})$ are obtained by eliminating all daggers in equation (28). In equation (27) the generalized Bessel functions $i_0^{00}\{f^0(r_{12}); f^1(r_{12})\}$ are [38]

$$i_0^{00}\{f^0(r_{12}); f^1(r_{12})\} = \frac{1}{2} \int_{-1}^1 dz i_0 \left(3 \left\{ [f^1(r_{12})]^2 + z^2 [f^0(r_{12})]^2 - z^0 [f^1(r_{12})]^2 \right\}^{1/2} \right) \quad (29)$$

where $i_0(x) = \sinh(x)/x$ is the spherical modified Bessel function of zero order.

The dashed line in figure 1 shows the inverse of the cluster size $(1/S^{EXP}(\rho))_{MSA}$ as given by equations (26)–(29). We observe that, in general, the mean cluster size is now dipole dependent but, in particular, the critical density ρ_c is the same as that for the extended hard spheres without dipoles.

3.2. GMSA-based EXP approximation

To have a dipole-dependent critical density we use an exponential approach that is based on a generalized mean spherical approximation [32]. In equation (21), we still take $d(\mathbf{1}, \mathbf{2}) = 0$, but now we consider that $h(\mathbf{1}, \mathbf{2})$ and $c(\mathbf{1}, \mathbf{2})$ verify the thermal Ornstein–Zernike equation closed by $h(\mathbf{1}, \mathbf{2}) = -1$ for $r_{12} < \sigma$ and

$$c(\mathbf{1}, \mathbf{2}) = K \frac{e^{-z(r_{12}-\sigma)}}{r_{12}} \Phi^{000}(\mathbf{1}, \mathbf{2}) + \beta \sqrt{\frac{10}{3}} \frac{\mu^2}{r_{12}^3} \Phi^{112}(\mathbf{1}, \mathbf{2}) \text{ for } r_{12} > \sigma \quad (30)$$

Here K and z are constants to be determined by requiring that, at contact, the reference part of $h(\mathbf{1}, \mathbf{2})$ and $dh(\mathbf{1}, \mathbf{2})/dr_{12}$ verify the quadratic version of the QHNC [33] for the hard dipoles. Thus equation (21) yields

$$g(\mathbf{1}, \mathbf{2}) = g_{0GMSA}(r_{12}; K(\mu), z(\mu)) \exp[h_{1MSA}(\mathbf{1}, \mathbf{2})] \quad (31)$$

where we explicitly indicate that, in the way they are determined, the GMSA parameters depend on the dipolar moment.

The QHNC relation we use to calculate K and z is

$$\begin{aligned} c^{000}(r_{12}) &= \exp \left[\eta^{000}(r_{12}) + \frac{1}{3} \left(\eta^{112}(r_{12}) - \beta \sqrt{\frac{10}{3}} \frac{\mu^2}{r_{12}^3} \right)^2 \right. \\ &\quad \left. + \frac{1}{6} \left(\eta^{110}(r_{12}) \right)^2 \right] - \eta^{000}(r_{12}) - 1 \end{aligned} \quad (32)$$

where $\eta \equiv h - c$. By evaluating equation (32) and its derivative at $r_{12} = \sigma^+$, we obtain a system of two algebraic equations for K and z .

$$K = h^{000}(\sigma) + \frac{1}{3}(h^{112}(\sigma))^2 + \frac{1}{6}(h^{110}(\sigma))^2 - \ln(h^{000}(\sigma) + 1) \quad (33)$$

$$z = \frac{1}{K} \left[\frac{h'^{000}(\sigma)}{h^{000}(\sigma) + 1} - h'^{000}(\sigma) - \frac{2}{3}h^{112}(\sigma)h'^{112}(\sigma) - \frac{1}{3}h^{110}(\sigma)h'^{110}(\sigma) \right] - 1 \quad (34)$$

where $h^{000}(\sigma)$ and $h'^{000}(\sigma)$ are functions of K and z [32].

From equation (31), in a similar form to that previously done of the MSA-based EXP connectedness pair correlation function, we obtain the corresponding $[h_{EXP}^\dagger(\mathbf{1}, \mathbf{2})]_{GMSA}$:

$$[h_{EXP}^\dagger(\mathbf{1}, \mathbf{2})]_{GMSA} = g_{GMSA}^{\dagger 000}(r_{12}) \exp[h_{1MSA}(\mathbf{1}, \mathbf{2})] + [g_{GMSA}^{000}(r_{12}) - g_{GMSA}^{\dagger 000}(r_{12})] \left\{ \exp[h_{1MSA}^\dagger(\mathbf{1}, \mathbf{2})] - 1 \right\} \quad (35)$$

The connectedness O-Z equation for the pair correlation function $g_{GMSA}^{\dagger 000}(r_{12})$ for extended hard spheres, when the thermal pair correlation function $g_{GMSA}^{000}(r_{12})$ verifies the O-Z equation with Yukawa closure $c(r_{12}) = Ke^{-z(r_{12}-\sigma)}/r_{12}$, has been solved by Xu and Stell [17].

The mean cluster size now reads

$$(S^{EXP})_{GMSA}(\rho) = 1 + 4\pi\rho \int_0^\infty dr_{12} r_{12}^2 \langle [h_{EXP}^\dagger(\mathbf{1}, \mathbf{2})]_{GMSA} \rangle_{\hat{\Omega}_1, \hat{\Omega}_2} \quad (36)$$

where $\langle [h_{EXP}^\dagger(\mathbf{1}, \mathbf{2})]_{GMSA} \rangle$ is given by the rhs of equation (27) by just changing $g_{MSA}^{000}(r_{12})$ and $g_{MSA}^{\dagger 000}(r_{12})$ to $g_{GMSA}^{000}(r_{12})$ and $g_{GMSA}^{\dagger 000}(r_{12})$, respectively.

The full line in figure 1 gives $(1/S^{EXP}(\rho))_{GMSA}$ versus ρ^* . The curve remarkably differs from that corresponding to extended hard spheres (dotted line) along the whole range of densities. In particular the critical density is smaller than the common value obtained in the MSA and the MSA-based EXP approximation (which, as was mentioned, does not depend on the dipolar moment) and practically coincides with the Monte Carlo result.

Figure 1 suggests that the GMSA-based EXP approximation is superior to the other two approximations. It also reproduces simulation results better than the connectedness first-order y -expansion considered in [29]. In order to have a more complete picture about the goodness of the approximation, in figure 2, we compare our results with Monte Carlo simulations for diverse values of the dipolar moment. Furthermore, in figure 3, the average $\langle [h_{EXP}^\dagger(\mathbf{1}, \mathbf{2})]_{GMSA} \rangle$ is checked against the corresponding simulation points. We see that our theory compares rather well with Monte Carlo calculations, especially at relatively low dipolar strengths.

As in previous work we also consider a ‘connectedness Kirkwood g factor’ defined as [29]

$$g_K^\dagger = 1 + \frac{\rho}{V} \int d\mathbf{1} d\mathbf{2} (\hat{\Omega}_1 \cdot \hat{\Omega}_2) h^\dagger(\mathbf{1}, \mathbf{2}) \quad (37)$$

This factor is proportional to the cluster average square dipolar moment. It provides a measure of the orientational ordering inside the clusters. In table 1, GMSA-based EXP results for g_K^\dagger are shown and compared with Monte Carlo data. Theoretical calculations were performed using

$$g_K^\dagger = 1 - 2\pi\rho \int_0^\infty dr_{12} r_{12}^2 g_{GMSA}^{\dagger 000}(r_{12}) J(r_{12}) - 2\pi\rho \int_0^\infty dr_{12} r_{12}^2 [g_{GMSA}^{000} - g_{GMSA}^{\dagger 000}](r_{12}) J^\dagger(r_{12}) \quad (38)$$

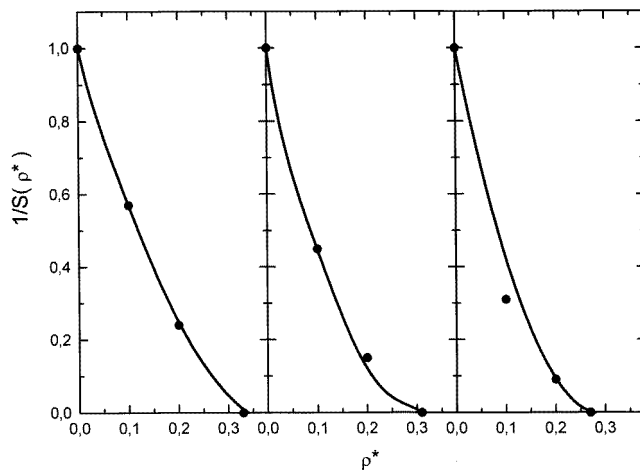


Figure 2. Inverse cluster size versus reduced density from the connectedness GMSA-based EXP approximation for diverse values of the reduced square dipolar moment. From left to right $\mu^{*2} = 1.0, 2.0, 2.75$. The full circles are the Monte Carlo results of [29].

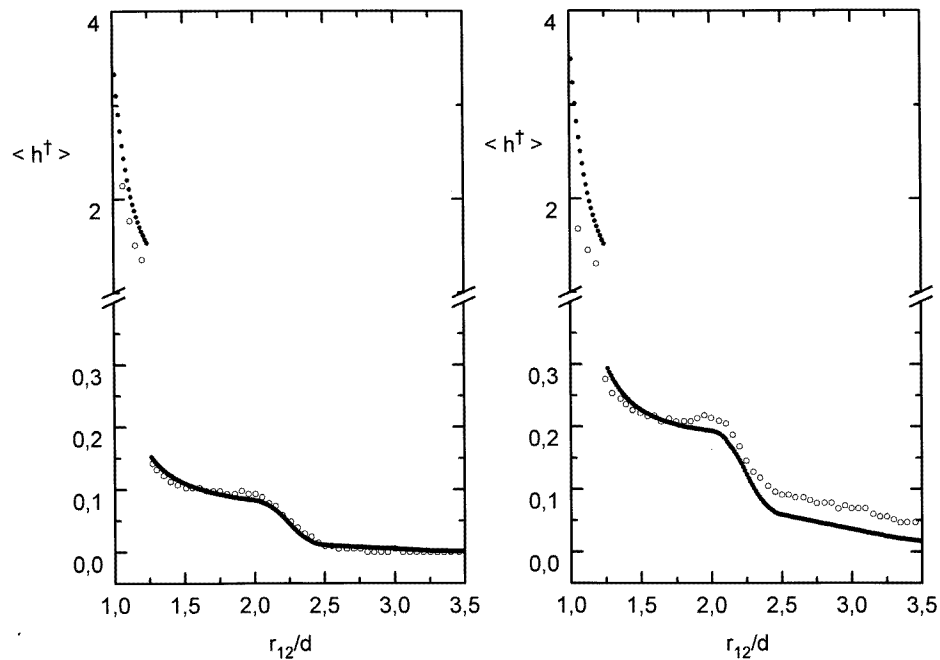


Figure 3. Angular-averaged connectedness pair-correlation function for the dipolar hard spheres system with $\mu^{*2} = 2.0$ from the GMSA-based EXP approximation. Left: $\rho^* = 0.1$; right: $\rho^* = 0.2$. The open circles are the Monte Carlo results of [29].

where

$$J^\dagger(r_{12}) = \int_{-1}^1 dz \frac{i_1 \left(3\sqrt{\left(h_{MSA}^\dagger(r_{12})\right)^2 + \left[\left(h_{MSA}^{\dagger 0}(r_{12})\right)^2 - \left(h_{MSA}^\dagger(r_{12})\right)^2\right]z^2} \right)}{\sqrt{\left(h_{MSA}^\dagger(r_{12})\right)^2 + \left[\left(h_{MSA}^{\dagger 0}(r_{12})\right)^2 - \left(h_{MSA}^\dagger(r_{12})\right)^2\right]z^2}}$$

$$\times \left[h_{MSA}^{\dagger 1}(r_{12}) - \left(h_{MSA}^{\dagger 0}(r_{12}) + h_{MSA}^{\dagger 1}(r_{12}) \right) z^2 \right] \quad (39)$$

and $J(r_{12})$ is obtained by eliminating all daggers in equation (39). In this last equation $i_1(x) = \cosh(x)/x - \sinh(x)/x^2$ is the modified spherical Bessel function of first order and functions $h_{MSA}^{\dagger 0}(r_{12})$ and $h_{MSA}^{\dagger 1}(r_{12})$ are given by equation (28). Equation (38) follows from equation (37) considering the expansion of Blum and Torruella again [38].

Table 1.

μ^{*2}	ρ^*	$(g_K^\dagger)_{GMSA-EXP}$	$(g_K^\dagger)_{MC}^a$	$(g_K^\dagger)_{YE}^a$
1.00	0.1	1.011	1.013	1.005
	0.2	1.026	1.038	1.012
2.00	0.1	1.070	1.076	1.055
	0.2	1.129	1.132	1.126
2.75	0.1	1.180	1.187	1.200
	0.2	1.219	1.211	1.454

^a $(g_K^\dagger)_{MC}$ and $(g_K^\dagger)_{YE}$ are from [29].

The GMSA-based EXP approximation compares with the results obtained from Monte Carlo simulations better than the other exponential approximations, particularly the connectedness y expansion [29].

4. Concluding remarks

In this work we have considered theoretical approaches to the continuum percolation of dipolar hard sphere fluids. In order to overcome an undesirable property, which is common to all linear theories, namely that mean cluster sizes do not depend on the particles dipolar moment, we propose to use the connectedness version of some exponential approximations.

Although a MSA-based exponential approximation, already considered in previous work, in general gives a mean cluster size that depends on the dipolar strength, it gives a critical density at the percolation transition that is the same as that for extended hard spheres without dipoles.

The second exponential approximation we introduce in this work, in contrast is dipolar dependent along the whole range of densities and compares rather well with Monte Carlo simulations. In the approximation, the reference part of the thermal pair correlation function is calculated using a generalized MSA where the Yukawa parameters are determined by demanding that the radial functions in the invariant expansion of the thermal pair correlation function and its first derivative are related at contact according to the quadratic version of the hypernetted chain approximation.

Acknowledgment

Support of this work by the Consejo Nacional de Investigaciones Científicas y Técnicas (CONICET) of Argentina is greatly appreciated.

References

- [1] Unger C and Klein W 1984 *Phys. Rev. B* **29** 2698
- [2] Coniglio A, Stanley H E and Klein W 1982 *Phys. Rev. B* **25** 6805
- [3] Tobochnik J, Gould H and Klein W 1986 *Phys. Rev. B* **33** 377
- [4] Stanley H E and Teixeira J 1980 *J. Chem. Phys.* **73** 3304
- [5] Simon S H, Dobrosavljević V and Stratt R M 1991 *J. Chem. Phys.* **94** 7360
- [6] Kirkpatrick S 1979 *Ill Condensed Matter (les Houches 1978)* ed R Balian, R Maynard and G Toulouse (Amsterdam: North-Holland)
- [7] Feldman Y, Kozlovich N, Nir I and Garti N 1995 *Phys. Rev. E* **51** 478
- [8] Stauffer D 1985 *Introduction to Percolation Theory* (London: Taylor and Francis)
- [9] Hill T L 1955 *J. Chem. Phys.* **23** 617
- [10] Coniglio A, De Angelis U, Forlani A and Lauro G 1977 *J. Phys. A: Math. Gen.* **10** 219
- [11] Coniglio A, De Angelis U and Forlani A 1977 *J. Phys. A: Math. Gen.* **10** 1123
- [12] Stell G 1984 *J. Phys. A: Math. Gen.* **17** L885
- [13] Chiew Y C and Glandt E D 1983 *J. Phys. A: Math. Gen.* **16** 2599
- [14] Chiew Y C, Stell G and Glandt E D 1985 *J. Chem. Phys.* **83** 761
- [15] DeSimone T, Demoulini S and Stratt R M 1986 *J. Chem. Phys.* **85** 391
- [16] Netemeyer S C and Glandt E D 1986 *J. Chem. Phys.* **85** 6054
- [17] Xu J and Stell G 1988 *J. Chem. Phys.* **89** 1101
- [18] Bug A L R, Safran S A and Webman I 1986 *Phys. Rev. B* **33** 4716
- [19] Sen A K and Torquato S 1988 *J. Chem. Phys.* **89** 3799
- [20] Hayes D M and Melrose J R 1989 *Mol. Phys.* **66** 1057
- [21] Gawlinski E T and Stanley H E 1981 *J. Phys. A: Math. Gen.* **14** 1291
- [22] Sevick E M, Monson P A and Ottino J 1988 *J. Chem. Phys.* **88** 6385
- [23] Seaton N A and Glandt E D 1987 *J. Chem. Phys.* **86** 4668
- [24] Bug L R, Webman I and Grest S A 1985 *Phys. Rev. A* **32** 506
- [25] Lee S B and Torquato S 1988 *J. Chem. Phys.* **89** 6427
- [26] Chiew Y C and Wang Y H 1988 *J. Chem. Phys.* **89** 6385
- [27] Deutscher G, Zallen R and Adler J (ed) 1983 *Annals of the Israel Physical Society* vol 3 (Jerusalem, Israel: Israel Physical Society)
- [28] Vericat F 1989 *J. Phys.: Condens. Matter* **1** 5202; 1990 *J. Phys.: Condens. Matter* **2** 3697
- [29] Laría D and Vericat F 1991 *Phys. Rev. A* **43** 1932
- [30] Andersen H C and Chandler D 1972 *J. Chem. Phys.* **57** 1918
- [31] Gubbins K E and Gray C G 1972 *Mol. Phys.* **23** 187
- [32] Hoye J S, Lebowitz J L and Stell G 1974 *J. Chem. Phys.* **61** 3253
- [33] Stell G, Patey G N and Hoye J S 1981 *Adv. Chem. Phys.* **38** 183
- [34] Wertheim M S 1971 *J. Chem. Phys.* **55** 4291
- [35] Blum L 1978 *J. Stat. Phys.* **18** 451
- [36] Hansen J P and McDonald I R 1976 *Theory of Simple Liquids* (London: Academic)
- [37] Cummings P T, Ram J, Barker R, Gray C G and Wertheim M S 1983 *Mol. Phys.* **48** 1177
- [38] Blum L and Torruella A J 1988 *J. Chem. Phys.* **89** 4976